

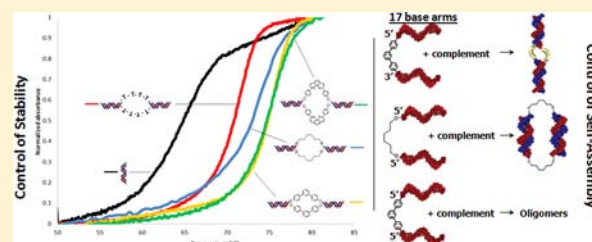
# The Role of Organic Linkers in Directing DNA Self-Assembly and Significantly Stabilizing DNA Duplexes

Andrea A. Greschner, Violeta Toader, and Hanadi F. Sleiman\*

Department of Chemistry and Center for Self-Assembled Chemical Structures (CSACS), McGill University, 801 Sherbrooke Street West, Montreal, QC H3A 2K6, Canada

**S** Supporting Information

**ABSTRACT:** We show a simple method to control both the stability and the self-assembly behavior of DNA structures. By connecting two adjacent duplexes with small synthetic linkers, factors such as linker rigidity and DNA strand orientation can increase the thermal denaturation temperature of 17 base-pair duplexes by up to 10 °C, and significantly increase the cooperativity of melting of the two duplexes. The same DNA sequence can thus be tuned to melt at vastly different temperatures by selecting the linker structure and DNA-to-linker connectivity. In addition, a small rigid *m*-triphenylene linker directly affects the self-assembly product distribution. With this linker, changes in the orientation of the linked strands (e.g., 5'3' vs 3'3') can lead to dramatic changes in the self-assembly behavior, from the formation of cyclic dimer and tetramer to higher-order oligomers. These variations can be readily predicted using a simple strand-end alignment model.



## INTRODUCTION

DNA is a powerful template to organize nanomaterials with precisely programmed features. Most current approaches in DNA nanotechnology, such as DNA tile assembly<sup>1–3</sup> or DNA origami,<sup>4,5</sup> use only DNA strands to guide the assembly process. We<sup>6–8</sup> and others<sup>9–12</sup> have demonstrated an alternative strategy that uses synthetic molecules as corner units and DNA strands as arms. This strategy allows the combination of the diverse structures and functions of organic molecules or transition metal complexes with the programmability of DNA. It has led to new methods of building DNA nanostructures that are DNA-economic and intrinsically dynamic, and that can display redox, photophysical, photochemical or catalytic activity.<sup>13–18</sup>

Here, we demonstrate that the structure and connectivity of synthetic organic linkers can play a major role in guiding the DNA self-assembly process, and can significantly stabilize the DNA duplexes in the resulting nanostructures (Scheme 1 and Chart 1). By attaching two identical DNA strands to short linkers in a 5' to 3' manner, self-assembled DNA dimers come together with significant increase in their thermal denaturation temperature ( $T_M$ ) as compared to separate DNA strands. A short and rigid triphenylene linker gives the greatest stabilization—a near 10 °C increase in  $T_M$ , and almost full cooperativity in the melting of its two duplexes.

A rigid organic linker also provides the ability to tune and dramatically modify the self-assembly outcome. 5'-3' connectivity leads to clean dimer formation, while 5'-5' connectivity does not give dimer at all, but instead leads to higher-order cycles and oligomeric assemblies. (Scheme 1b). The outcome is different when flexible corner units are used,

which give dimers for all connectivities (Scheme 1c). We propose a mechanism where the assembly is directed by strand-end orientation, and we use this mechanism to successfully predict the assembly outcome of a system with shorter DNA strands.

Changing the duplex connectivity permitted further tuning of the  $T_M$ 's of each dimer—up to 5 °C, an effect that could be used to create DNA nanostructures with varied melting temperatures without changing the sequences.

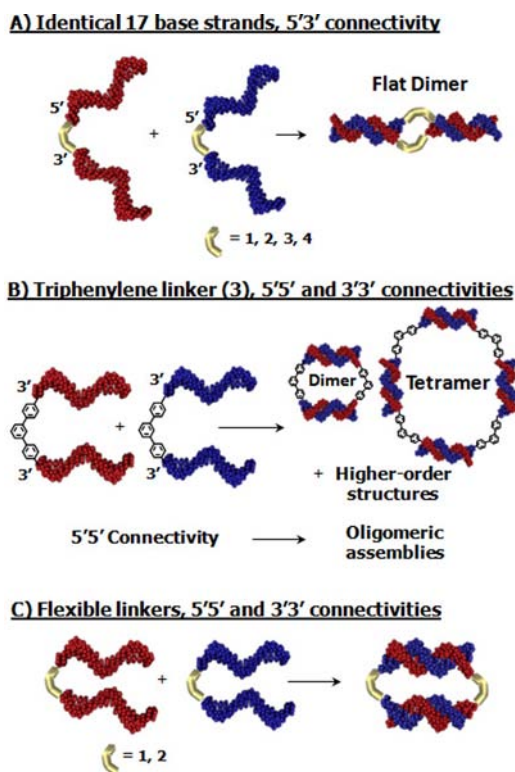
Previous reports from the groups of Mirkin, Nguyen, and Schatz have shown that gold nanoparticles<sup>19–22</sup> or polymers<sup>14,21–24</sup> decorated with multiple neighboring DNA strands can display increased cooperativity in their melting transitions and increased melting temperatures. Recently as well, 'caged dimers' that are linked together by longer and more flexible organic linkers displayed increased cooperativity in their melting transitions.<sup>12,25,26</sup> The present study demonstrates that, when smaller and more rigid organic linkers with the proper strand orientation are used to link two DNA strands, significant stabilization can be obtained, comparable now to aggregates with multiple DNA strands. In addition, the nature and connectivity of the linker can directly influence the DNA self-assembly outcome in a predictable manner.

This study provides new structural parameters that can be readily used in DNA nanotechnology. Instead of relying on a large number of different DNA sequences to prevent self-assembly errors, the structure of the organic linker and its connectivity can be used to tune the assembly process, while

Received: April 10, 2012

Published: August 8, 2012

Scheme 1. (a) With Organic Linkers Connecting Two Identical 17-Base DNA Strands in a 5'-3' Manner, Assembly Gives a Flat Dimer; (B) Triphenylene Linker 3 Gives Different Structures for Different Connectivities; (C) Flexible Linkers 1 and 2 Assemble to Give Dimers Regardless of the Connectivity



keeping the DNA strands identical in sequence. Varying the structure and connectivity of the linker also allows the thermal denaturation temperature of the same DNA sequence to be tuned to widely different values.

Fundamentally, this work and the work cited above emphasize that using common databases to estimate the melting temperatures of DNA duplexes in more complex assemblies (based only on sequence and salt conditions) can be misleading. Depending on their connectivity, duplexes in close proximity can strongly interact with each other, leading to large differences in their thermal denaturation behavior from that estimated for individual duplexes.

## RESULTS AND DISCUSSION

**Dimer Assembly with 5'3' Connectivity.** For this series of experiments, two DNA duplexes were connected with linkers 1–4, where 1 is a flexible hexane-diol (C6) linker, 2 is a DNA-based four-thymidine (T4) linker, 3 is a rigid *m*-triphenylene organic linker, and 4 is a rigid 2,9-diphenyl-1,10-phenanthroline linker (Chart 1).<sup>17,27</sup> Each linker was attached to two 17-base single-stranded DNA arms of identical sequence (A'), with 5'3' connectivity. When combined with its complement (A''), only one structure was observed via PAGE analysis, with a mobility corresponding to a dimer (Figure 1). The identity of the bands in Figure 1 as fully double stranded dimers was confirmed with control experiments (see Supporting Information [SI]). Due to the use of identical DNA strands, there can be two possible assembly outcomes for dimers of 5'3' connectivity—cyclic dimers (cycA) and flat dimers (flatA) as shown in Scheme 2.

Chart 1. Four Linkers Studied in This Work: (1) Hexane-Diol Linker 1 (2) Four-Thymine DNA Linker 2, (3) *m*-Triphenylene Rigid Organic Linker 3, (4) Diphenylphenanthroline Linker 4; (Right) Three Possible DNA-to-Linker Connectivities, 5'-3', 5'-5', and 3'-3'

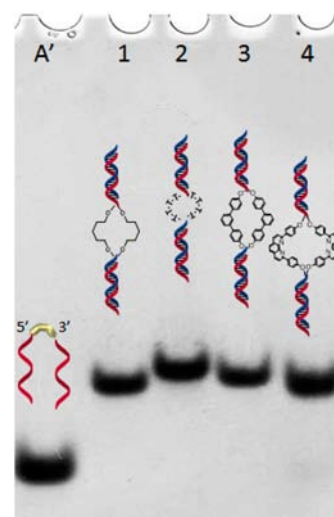
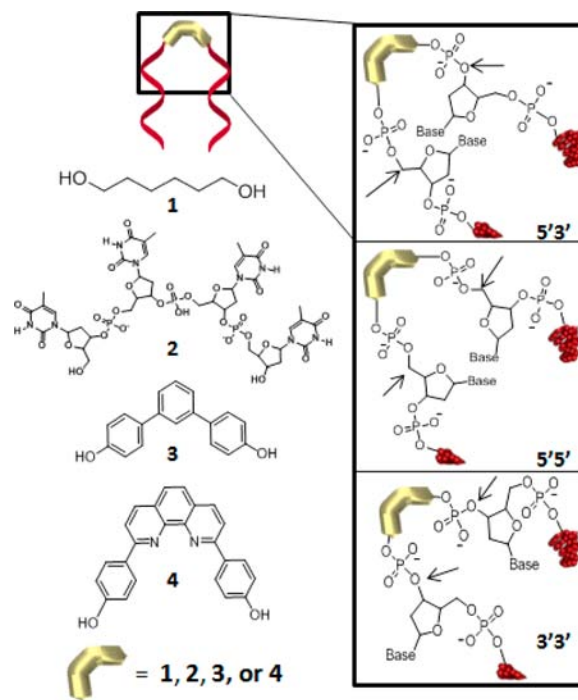


**Figure 1.** Assembly of 5'3'-connected dimers with each of 4 linkers. Far left: A' monomer. Lane 1: hexane diol linker 1. Lane 2: T4 DNA-based linker 2. Lane 3: Rigid triphenylene linker 3. Lane 4: Rigid diphenylphenanthroline linker 4.

A number of experiments were used to distinguish which dimer was formed. First, a FRET experiment was designed. Strand 2A' was modified with an Epoch Eclipse quencher at the 3' end and a Yakima Yellow fluorophore at the 5' end (F2A', Figure 2, see SI for more detail).<sup>28</sup> In the flat dimer, the fluorophore and quencher would be rigidly oriented at opposite ends of the structure, resulting in unquenched fluorescence. In contrast, in the cyclic structure, the fluorophore would be spatially oriented near the quencher, resulting in a decrease in

**Scheme 2. Two Possible Dimer Formations When the 17-Base DNA Arms Are Identical (A system), a Cyclic (cycA), and a Flat (flatA) Dimer**

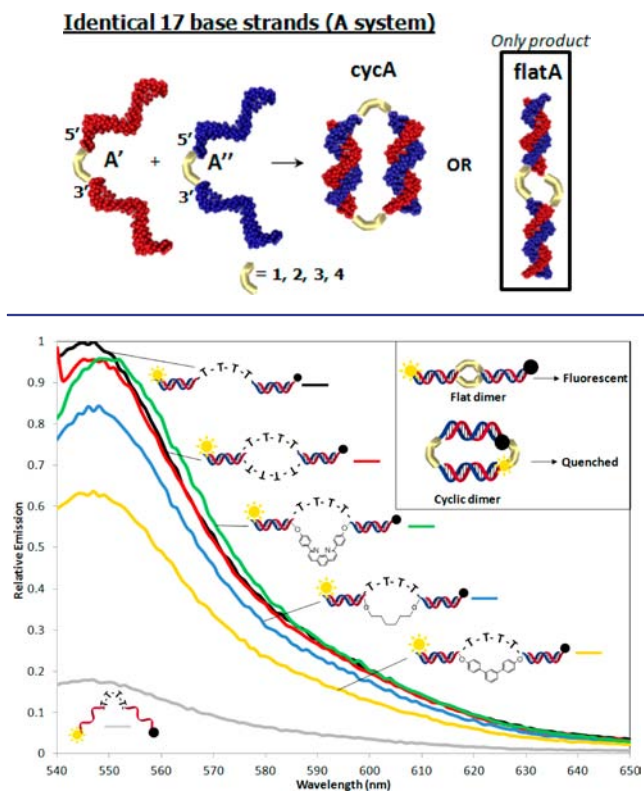


**Figure 2.** FRET measurements indicate that the 5'3' dimer assembly most closely resembles a flat dimer. The black curve represents a control consisting of a rigidified F2A' strand. The red curve is the dimer F2A. The green curve is a dimer of F2A' and 4A''. The blue curve is a dimer of F2A' and 1A''. The yellow curve is a dimer of F2A' and 3A''. The gray curve is F2A'.

overall fluorescence (Figure 2 inset). Two controls were used in this experiment. First, the F2A' strand was hybridized with two strands that are complementary to its two arms (Figure 2, black trace). This is expected to separate the FRET pair to a distance comparable to that of a flat dimer. Second, the F2A' strand in its single-stranded form was used to estimate a closer distance for the FRET pair and increased quenching, due to its flexible nature (Figure 2, grey trace). Against these two controls, the 17mer strands with 5'3' connectivity showed higher fluorescence values in the range expected for a flat dimer, for all linkers. A decrease in fluorescence intensity with dimers that place small linkers 1 and 3 face-to-face with the larger T4 linker in F2A' is likely due to increased bending as a result of the linker size mismatch, thus bringing the fluorophore closer to the quencher. Overall, this first set of experiments is consistent with formation of flat dimers as the preferred assembly outcome for the 5'3' connectivity.

In a second experiment, we attempted to generate an authentic sample of a cyclic dimer from linker 3 (see below), using DNA strands of different sequence. Unlike the clean dimer formation observed earlier (Figure 1, lane 3), this experiment yielded product mixtures, which further supports the identity of the structures in Figure 1 as flat dimer.

Finally, we took advantage of the metal-binding properties of linker 4. This linker is capable of binding copper(I) when two

ligands are oriented toward one another—as in the flat dimer (Figure 3a). In the cyclic orientation (Scheme 2), the two

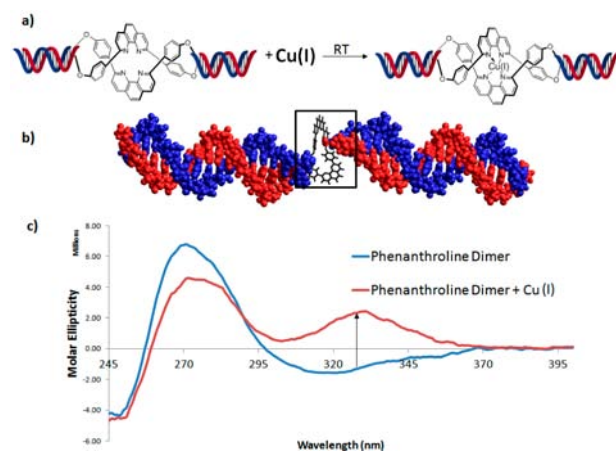


**Figure 3.** (a) In the flat dimer orientation, the diphenylphenanthroline moieties are near enough to bind copper(I). (b) Molecular modeling of the flat dimer indicates that the diphenylphenanthrolines are positioned such that copper can bind (see SI). (c) Circular dichroism shows an increase at ~330 nm, characteristic of copper(I) binding.

phenanthroline linkers are separated by the length of a 17 base pair duplex, and copper coordination to both would be unfavorable. The binding of copper [Cu(CH<sub>3</sub>CN)<sub>4</sub>][PF<sub>6</sub>]<sub>2</sub> to pre-annealed structures was monitored at room temperature using circular dichroism (CD). Figure 3c clearly shows an increase in the CD trace at 330 nm, characteristic of copper binding,<sup>29</sup> suggesting flat-dimer assembly. In contrast, when we generated a flat dimer where the phenanthroline linker is face-to-face with the 4-thymidine linker 2, no copper coordination was detected by CD (see SI).

**Effect of Linker on Dimer Stability.** Having determined the assembly outcome of 5'3' linker connectivity, we proceeded to study the relative effect of each linker on DNA stability. Results of the thermal denaturation analysis are given in Figure 4 and Table 1. It is clear that linking the two duplexes into a dimer results in a substantial increase in stability in comparison

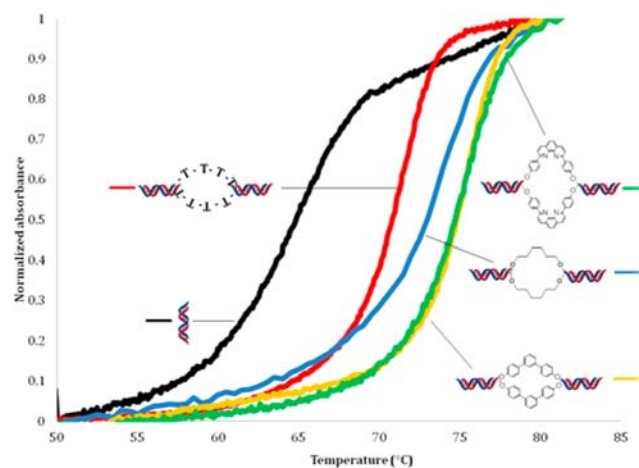


**Figure 4.** Thermal denaturation of the A system with each of the four linkers. The black curve represents a single duplex (control). The red curve is the dimer with linker 2. The blue curve is the dimer with linker 1. The yellow curve is the dimer with linker 3, and the green curve is the dimer with linker 4.

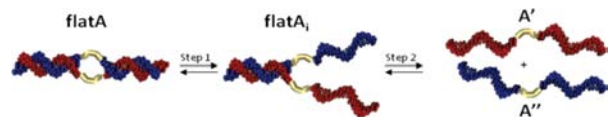
Table 1. Thermal Denaturation Results for Linkers

linker	$T_M$ (°C)	$\Delta T_M$ (°C)	fwhm (°C)	$\Delta H$ (kJ/mol)
single 17mer duplex	64.6 ± 0.8	0	8.5	540 ± 4
1	72.5 ± 0.6	7.9	4.2	780 ± 20
2	71.6 ± 0.7	7.0	4.6	830 ± 20
3	74 ± 1	9.6	3.2	1050 ± 20
4	74.6 ± 0.3	10.0	4.7	810 ± 10
single 34 mer duplex	79.0 ± 0.5	14.4	3.1	1250 ± 20

to a single duplex. For all linkers, we observe a significant increase in  $T_M$ , accompanied by a drastic decrease in full width at half-maximum (fwhm), which is a measure of melting cooperativity.<sup>12,19,21,23</sup> In particular, use of the rigid linkers 3 and 4 result in the greatest increase in  $T_M$  of up to 10 °C with a corresponding decrease in fwhm from 8 °C → 3 °C and 8 °C → 4.7 °C respectively.

The melting behavior of the two duplexes can be understood as a composite of two types of phenomena: allosteric and chelate cooperativity.<sup>30</sup> We hypothetically consider the melting of dimer A, or the reverse association of strands A' and A'' as a two-step process, as shown in Scheme 3.

### Scheme 3. Hypothetical Two-Step Melting of Flat DNA Duplex Dimers



Allosteric cooperativity refers to a favorable interaction between the two duplexes in dimer A, which can make dissociation of the first duplex (step 1) more difficult than dissociation of the second duplex (step 2). The small linkers used in this study appear to allow a favorable interaction between the two duplexes, such that their melting begins to resemble that of a 34mer duplex instead of two separate 17mer duplexes. This can explain both the observed increase in  $T_M$  and the narrowing of the melting curve, as measured by the full width at half-maximum. The first duplex begins denaturation at a higher temperature, because of the additional stabilization mediated by the small linker (**flatA**, Scheme 3). Now the system is at a much higher temperature than that required to melt the second duplex, and with the linkers still attached to already melted strands, the second duplex will denature very rapidly (step 2, Scheme 3), resulting in a narrow fwhm (Table 1).

Chelate cooperativity can best be understood by following the reverse association process in Scheme 3. As strands A' and A'' come together, a transient structure **flatA<sub>i</sub>** is formed. Association of the second pair of complementary strands in **flatA<sub>i</sub>** is now intramolecular and depends on the effective concentration of these two strands. This effective concentration is highly sensitive to the geometry of the linkers between the duplexes. The smaller and more rigid the linkers, the more preorganized the two strands in this intermediate structure. This leads to a higher effective concentration of the two strands, and a greater proportion of the fully bound dimer A.

Aromatic, rigid linkers 3 and 4 give the greatest stabilization with  $\Delta T_M = 9.6$  and 10 °C respectively. 3 is arguably the best, exhibiting the steepest melting curve (fwhm = 3.2 °C) and greatest change in enthalpy ( $\Delta H = 1050$  kJ mol<sup>-1</sup>), indicating

that its two duplexes are melting almost simultaneously. Linkers 3 and 4 can undergo  $\pi$ - $\pi$  stacking when they are oriented in a face-to-face manner in the dimer (Scheme 2), thus increasing the hybridization enthalpy, as well as further mediating the interaction between the two duplexes and contributing to allosteric cooperativity. In addition, their rigidity and small size result in a large degree of preorganization, which contributes to chelate cooperativity. Because the  $T_M$  of a duplex is logarithmically related to the initial concentration of single-stranded DNA, a  $\Delta T_M$  of 10 °C for **3flatA** implies a large effective concentration of the single-strands of intermediate structure A<sub>i</sub> (estimated to be approximately 800  $\mu$ M, when 5  $\mu$ M strands A' and A'' are used, see SI). The small and rigid *m*-triphenylene linker 3 significantly increases chelate cooperativity, by preorganizing the two single strands of intermediate A<sub>i</sub> and confining them to a highly reduced effective volume.

Significant  $T_M$  increases have been demonstrated for aggregates linked with multiple duplexes down to a minimum of three.<sup>26</sup> Recently, the groups of Nguyen and Schatz<sup>26</sup> demonstrated that trimers linked by aromatic vertices and assembled in a face-to-face (flat) manner result in higher  $T_M$ 's than the same trimers assembled as caged duplexes. The observed increases were attributed primarily to  $\pi$ - $\pi$  stacking interactions between the linkers.

Interestingly, in the present work, we found that flexible linkers 1 and 2 both significantly raised the melting temperature of the system over that of the single duplex, with significant increases in cooperativity. In particular, small aliphatic linker 1, that is unable to  $\pi$ -stack, shows a significant increase of 8 °C (Table 1). These results imply that, although  $\pi$ -stacking of linkers can play an important role, it is not required for stabilization of two linked duplexes. A compact linker, even when nonaromatic, can significantly contribute to both allosteric and chelate cooperativity, resulting in increases in  $T_M$  and fwhm.

Overall, this implies that using small and structurally well-defined linkers provides a simple method to significantly increase the stability and melting cooperativity of DNA duplexes without modifying the sequences of the strands.

**Effect of DNA-to-Linker Connectivity on Stability.** To investigate the importance of DNA-to-linker connectivity on assembly outcome, DNA strands with different connectivities were made. The connectivity is named according to the DNA strand-end that is attached to the linker, i.e. 5'5' refers to a strand with the directionality 3'-5'-L-5'-3', where L = 1, 2, or 3 (Chart 1). See Table S1 (SI) for sequences used. Each complementary pair of strands is capable of assembling into a wide array of structures, including dimer, trimer, tetramer, etc.

As shown earlier, all molecules with 5'3' connectivity and identical strands preferentially assemble into flat dimers. In contrast, the 5'5' or the 3'3' strands are not capable of forming flat dimers, and because of their strand polarity they only give cyclic structures when all their available strands are bound. Thus, in order to better compare these connectivities, we moved to a system B containing nonidentical strands of similar melting temperature, such that all connectivities uniformly lead to cyclic structures when fully bound, and flat dimer is prevented, as shown in Scheme 4 (see SI for system A with 5'5'/3'3' connectivity and identical sequences).

First, B' and B'' strands with the desired connectivities were annealed, and the resulting structures were analyzed by PAGE (Figure 5). This shows that flexible linkers 1 and 2 consistently form cyclic dimers for all connectivities. Interestingly, the

**Scheme 4. Assembly of 17 Base Strands with Flexible Linkers; Each DNA Arm Is Unique and Flexible Linkers Assemble to Form Cyclic Dimers**

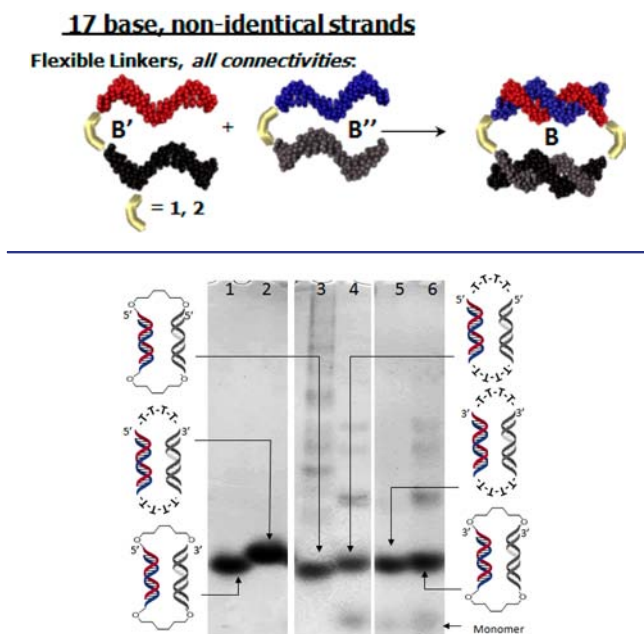


**Figure 5.** PAGE analysis of dimers of linkers 1 and 2 with each possible connectivity. Lanes: (1) 1A 5'3', (2) 2A 5'3', (3) 1A 5'5', (4) 2A 5'5', (5) 1A 3'3', (6) 2A 3'3'.

product distribution for linker 3 changes dramatically with differing connectivities, which will be discussed later. Thermal denaturation information for DNA-to-linker connectivity studies (Table 2) will thus focus on linkers 1 and 2. Because

**Table 2. Effect of Connectivity on Thermal Stability**

Linker	Connectivity	$T_M$ ( $^{\circ}\text{C}$ )	fwhm ( $^{\circ}\text{C}$ )	$\Delta H$ (kJ/mol)
single duplex CA	N/A	$64.6 \pm 0.8$	7.8	$472 \pm 6$
single duplex CB	N/A	$61.6 \pm 0.3$	8.2	$467 \pm 4$
1B	5'3'	$67.5 \pm 0.2$	4.5	$580 \pm 10$
	5'5'	$67.2 \pm 0.6$	5.4	$400 \pm 7$
	3'3'	$65.6 \pm 0.3$	5.9	$518 \pm 9$
2B	5'3'	$67.4 \pm 0.4$	4.6	$590 \pm 20$
	5'5'	$66.6 \pm 0.2$	6.0	$321 \pm 6$
	3'3'	$62.9 \pm 0.1$	>7.8	$359 \pm 5$

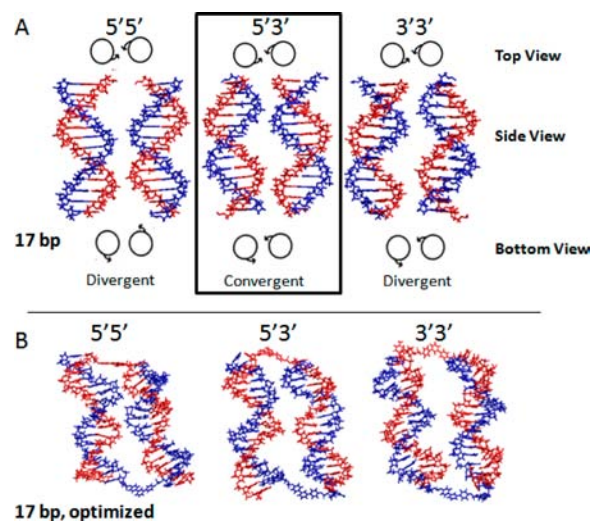
the two DNA strands in B' and B'' have different sequences, the results of Table 2 should be considered qualitatively (SI provides the full thermal denaturation results for the 5'5' and 3'3' connectivities with identical DNA strands).

As the connectivity is changed from 5'3' to 5'5' and 3'3', a steady decrease in  $T_M$ , increase in fwhm, and decrease in  $\Delta H$  are observed, to a point where the 3'3' system melts more like two independent duplexes (see also SI). This decrease in stability is also apparent in the PAGE analysis in Figure 5. In the 5'3' connectivity, formation of dimer is quantitative for both linkers. However, both 3'3' and 5'5' connectivities are lower yielding, with some nonhybridized monomers and higher-order structures as side products.

One factor that can possibly contribute to the destabilization of some of the cyclic dimers is DNA strand-end alignment. If the two duplexes were only connected by a linker at one end, or

in a flat configuration, no strain would be expected upon binding. However, by tethering the duplexes at both ends with structurally small linkers, strain is likely induced, and would be relieved by over- or under-winding of the duplexes, and/or fraying of the duplex ends. Scheme 5 shows a schematic model

**Scheme 5. (a) 17bp System;<sup>a</sup> (b) Optimized Models for a Cyclic Dimer (17 Bases Per Duplex, with Linker 3)<sup>b</sup>**



<sup>a</sup>The red DNA strand-ends are ideally aligned at the top of the duplex. Underneath, directional arrows show how the DNA strand-ends would align (blue DNA). <sup>b</sup>Models minimized using AMBER forcefield, Hyperchem 8.0.

of the strand-end alignment, illustrating how two linkers would subtend the top and bottom duplex ends (circles with arrows). Each duplex was rotated about its long axis such that the top linker could easily bridge the distance between the two duplexes. A bottom view shows how the DNA strand-ends would then be oriented for binding the second linker. For 17bp duplexes (Scheme 5), these models show that 5'3' connectivity possesses a better DNA strand-end alignment for linker binding. Conversely, 3'3' and 5'5' dimers would need to distort to allow the linker to bridge the duplex ends. Further evidence for the role of strand-end alignment is given below, using the rigid linker 3.

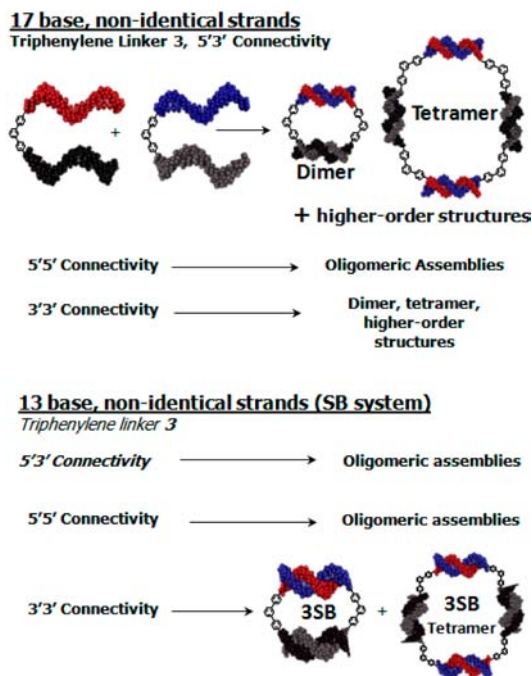
**Effect of Rigid Linker and DNA-to-Linker Connectivity on DNA Self-Assembly.** Based on the strand-end alignment problem, a greater degree of duplex strain and distortion is expected for the 5'5' and 3'3' connectivity, as is manifested by the thermal denaturation data and PAGE analysis for linkers 1 and 2. Both linkers are relatively flexible, and would be conformationally mobile enough to somewhat relieve this strain, leading to the high dimer yields in Figure 5. On the other hand, linker 3 is much more rigid and would therefore not be as readily distorted to relieve this strain. 3 is smaller than any previously reported synthetic linker, allowing it to hold the duplexes closer together and increasing their interactions.

To promote formation of cyclic structures for all connectivities of linker 3, we again constructed a B system with two distinct 17 base arms (see SI for PAGE and thermal denaturation results for connectivities with identical DNA strands).

Interestingly, we find that linker 3 gives a dramatically different assembly outcome, as compared to the more flexible

linkers 1 and 2 (Scheme 6). PAGE analysis (Figure 6) shows that the 5'5' connectivity for 3 gives no dimers. Instead, larger,

**Scheme 6. (Top) Assembly Outcome for the Rigid Triphenylene Linker 3 in the 17-Base System; Different Connectivities Result in Different Structural Distributions; (Bottom) Assembly Outcome for the Rigid Triphenylene Linker 3 in the 13 Base System; Structural Distribution Has Changed**



nongel penetrating oligomers are observed. The result for 3'3' shows a well-resolved ladder of distinct structures ranging from dimer to octamer with the bulk of the assemblies (~40%) present as nonpenetrating oligomer. The characterization of the discrete structures as cyclic, closed assemblies is supported by experiments shown in the SI. The 5'3' connectivity for linker 3 gives a number of cyclic structures, although dimer is the main product (~30%), and very little nongel-penetrating oligomer is formed. Linker 3 thus appears to favor the formation of higher-order oligomers and prevents the formation of small cyclic assemblies for the 5'5' and 3'3' connectivities. While it gives a more significant proportion of dimer for the 5'3' connectivity, the assembly outcome is very different from the flexible linkers 1 and 2, which result in dimers for all connectivities.

To explain these findings, we performed preliminary molecular modeling studies of the cyclic dimers with linker 3 (Scheme 5b). These suggest that the 5'3' connectivity results in less duplex distortion than the 5'5' and 3'3' dimers, consistent with better strand-end alignment (Figure 5b). However there is still fraying of the duplexes with this more favorable 5'3' connectivity, due to the reduced size and lack of conformational mobility in the triphenylene linker 3. These studies confirm that, by choosing a specific linker structure and connectivity, one can dramatically change DNA self-assembly.

To further investigate how strand-end alignment influences self-assembly products, a new, shorter system was developed, SB, this time with 13 base-pairs per duplex, reducing the total number of helical turns (Schemes 6 and 7). The 13bp duplex length was predicted to show optimal strand-end alignment for

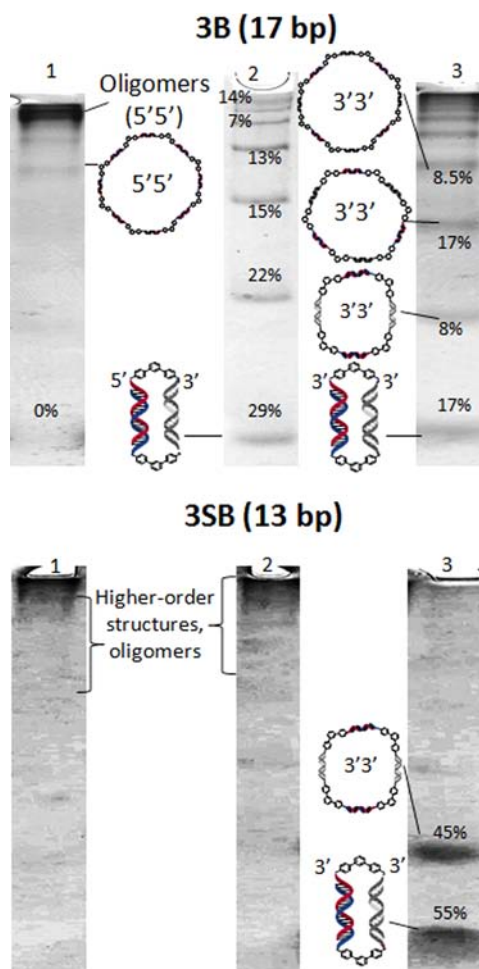
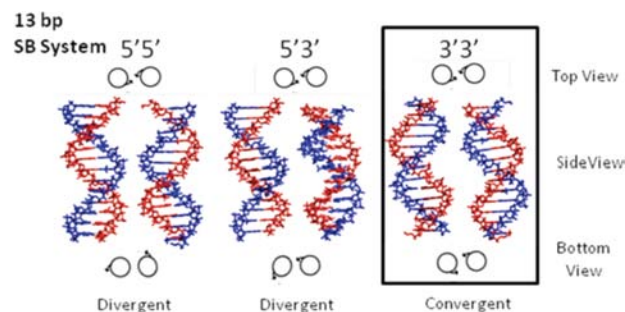


**Figure 6.** Structural distribution for assemblies of rigid vertex 3, with: Lanes 1, 5'5' connectivity. Lanes 2, 5'3' connectivity. Lanes 3, 3'3' connectivity. *Top* system B with distinct DNA 17 base arms. *Bottom* system B with 13 base arms.

**Scheme 7. Strand-End Alignment Analysis Predicts That 3'3' DNA-to-Linker Connectivity Will Be Favored in a 13bp System**



the 3'3' connectivity, rather than the 5'3' connectivity—opposite the trend of the 17bp rigid linker system (Scheme 5a).

Again, the rigid linker 3 was used since it is sensitive to changes in connectivity. On the basis of simple models (Scheme 7), the 3'3' connectivity appears most favorable in allowing the linkers to bridge the top and bottom strand-ends. If DNA strand-end orientation is indeed a driving factor in determining self-assembly products, a shift in product distribution toward smaller structures should be observed for

this connectivity. Interestingly, a significant shift is observed. By changing the number of bases, product distribution was changed from higher-order structures to only two small products, namely the dimer and the tetramer (Figure 6, bottom, Scheme 6). In addition, where before only 17% of the structures formed were dimer and the major product (41%) was oligomeric, 3'3' dimer is now one of the two principal products (55% yield). Conversely, where 5'3' connectivity previously yielded smaller cyclic structures, we now see the defined structures disappear completely, leaving only oligomeric assemblies. The assignment of the gel electrophoresis bands as closed dimers and tetramers is supported by a number of experiments that are described in the Supporting Information.

This data supports the conclusion that, for the small linker systems, strand-end-orientation is an important factor in determining which DNA-to-linker connectivity provides the greatest increase in stability. This can be readily predicted by simple modeling such as that shown in Schemes 5 and 7.

Understanding the effect of DNA-to-linker connectivity provides an extra dimension of tunability when designing DNA structures. Connectivity can be used to fine-tune  $T_m$  by an additional 7 °C, as well as provide a method to obtain different self-assembled products, such as dimers or tetramers rather than oligomers.

## CONCLUSIONS

We have shown a simple method to control both the stability and the self-assembly behavior of DNA structures. By using small, synthetic linkers that connect two adjacent duplexes, factors such as linker size, rigidity and connectivity can increase the thermal denaturation temperature of 17-base pair duplexes by up to 10 °C and significantly narrow the melting profile of the two duplexes. For the same DNA sequence, one can now tune the melting temperature to vastly different values by selecting the linker structure and DNA-to-linker connectivity.

Furthermore, a small rigid linker can be used to directly affect the self-assembly product distribution. Because of the strict requirements that it imposes, subtle changes in the orientation of the linked strands (e.g., 5'3' vs 3'3') can now lead to dramatic changes in the self-assembly behavior. These variations can be readily predicted using a simple strand-end alignment model.

Incorporation of these linkers into DNA strands is a very simple, on-column, and high-yielding process. We anticipate the usefulness of this method in DNA nanotechnology, where the melting temperature of the same DNA sequence can now be rationally varied and controlled with simple structural modifications of the duplex linkers.

Fundamentally, this study contributes further insight into DNA interduplex interactions, which are important in chromosome packaging and homologous recombination. In addition, the large increase in stability and melting cooperativity of short duplexes will find a number of applications in biotechnology, such as in more sensitive DNA detection and diagnostics.

## ASSOCIATED CONTENT

### Supporting Information

Detailed methods, DNA sequences, quantitative analysis, additional figures. This material is available free of charge via the Internet at <http://pubs.acs.org>.

## AUTHOR INFORMATION

### Corresponding Author

hanadi.sleiman@mcgill.ca

### Notes

The authors declare no competing financial interest.

## ACKNOWLEDGMENTS

We thank FQRNT, NSERC, CFI, CIHR, and CSACS for financial support, and Faisal Aldaye for the basic design of the symmetrical assembly system.

## REFERENCES

- (1) Lin, C.; Liu, Y.; Rinker, S.; Yan, H. *ChemPhysChem* **2006**, *7*, 1641–1647.
- (2) Seeman, N. C. *J. Theor. Biol.* **1982**, *99*, 237–247.
- (3) Sobey, T. L.; Renner, S.; Simmel, F. C. *J. Phys.: Condens. Matter* **2009**, *21*, 034112.
- (4) Andersen, E. S.; Dong, M.; Nielsen, M. M.; Jahn, K.; Lind-Thomsen, A.; Mamdouh, W.; Gothelf, K. V.; Besenbacher, F.; Kjems, J. *ACS nano* **2008**, *2*, 1213–1218.
- (5) Andersen, E. S.; Dong, M.; Nielsen, M. M.; Jahn, K.; Subramani, R.; Mamdouh, W.; Golas, M. M.; Sander, B.; Stark, H.; Oliveira, C. L. P.; Pedersen, J. S.; Birkedal, V.; Besenbacher, F.; Gothelf, K. V.; Kjems, J. *Nature* **2009**, *459*, 73–U75.
- (6) Yang, H.; Altvater, F.; de Bruijn, A. D.; McLaughlin, C. K.; Lo, P. K.; Sleiman, H. F. *Angew. Chem., Int. Ed.* **2011**, *50*, 4620–4623.
- (7) McLaughlin, C. K.; Hamblin, G. D.; Sleiman, H. F. *Chem. Soc. Rev.* **2011**, *40*, 5647–5656.
- (8) Aldaye, F. A.; Sleiman, H. F. *J. Am. Chem. Soc.* **2007**, *129*, 13376–13377.
- (9) Shi, J.; Bergstrom, D. E. *Angew. Chem., Int. Ed.* **1997**, *36*, 111–113.
- (10) Zimmermann, J.; Cebulla, M. P. J.; Mönninghoff, S.; von Kiedrowski, G. *Angew. Chem., Int. Ed.* **2008**, *47*, 3626–3630.
- (11) Scheffler, M.; Dorenbeck, A.; Jordan, S.; Wüstefeld, M.; von Kiedrowski, G. *Angew. Chem., Int. Ed.* **1999**, *38*, 3311–3315.
- (12) Eryazici, I.; Prytkova, T. R.; Schatz, G. C.; Nguyen, S. T. *J. Am. Chem. Soc.* **2010**, *132*, 17068–17070.
- (13) Yoshizawa, M.; Fujito, M. *Pure Appl. Chem.* **2005**, *77*, 1107–1112.
- (14) Gibbs, J. M.; Park, S.-J.; Anderson, D. R.; Watson, K. J.; Mirkin, C. A.; Nguyen, S. T. *J. Am. Chem. Soc.* **2005**, *127*, 1170–1178.
- (15) Lo, P. K.; Karam, P.; Aldaye, F. A.; McLaughlin, C. K.; Hamblin, G. D.; Cosa, G.; Sleiman, H. F. *Nat. Chem.* **2010**, *2*, 319–328.
- (16) Seeman, N. C. *Nature* **2003**, *421*, 427–431.
- (17) Yang, H.; McLaughlin, C. K.; Aldaye, F. A.; Hamblin, G. D.; Rys, A. Z.; Rouiller, I.; Sleiman, H. F. *Nat. Chem.* **2009**, *1*, 390–396.
- (18) Yang, H.; Metera, K. L.; Sleiman, H. F. *Coord. Chem. Rev.* **2010**, *254*, 2403–2415.
- (19) Jin, R.; Wu, G.; Li, Z.; Mirkin, C. A.; Schatz, G. C. *J. Am. Chem. Soc.* **2003**, *125*, 1643–1654.
- (20) Long, H.; Kudlay, A.; Schatz, G. C. *J. Phys. Chem. B* **2006**, *110*, 2918–2926.
- (21) Lytton-Jean, A. K. R.; Gibbs-Davis, J. M.; Long, H.; Schatz, G. C.; Mirkin, C. A.; Nguyen, S. T. *Adv. Mater.* **2009**, *21*, 706–709.
- (22) Park, S. Y.; Gibbs-Davis, J. M.; Nguyen, S. T.; Schatz, G. C. *J. Phys. Chem. B* **2007**, *111*, 8785–8791.
- (23) Gibbs-Davis, J. M.; Schatz, G. C.; Nguyen, S. T. *J. Am. Chem. Soc.* **2007**, *129*, 15535–15540.
- (24) Kudlay, A.; Gibbs, J. M.; Schatz, G. C.; Nguyen, S. T.; Olvera de la Cruz, M. *J. Phys. Chem. B* **2007**, *111*, 1610–1619.
- (25) Stepp, B. R.; Gibbs-Davis, J. M.; Koh, D. L. F.; Nguyen, S. T. *J. Am. Chem. Soc.* **2008**, *130*, 9628–9629.
- (26) Eryazici, I.; Yildirim, I.; Schatz, G. C.; Nguyen, S. T. *J. Am. Chem. Soc.* **2012**.
- (27) Aldaye, F. A.; Sleiman, H. F. *J. Am. Chem. Soc.* **2007**, *129*, 10070–10071.

- (28) Lukhtanov, E. A.; Metcalf, M.; Reed, M. W. *Am Biotechnol Lab* **2001**, *19*, 68–69.
- (29) Yang, H.; Altvater, F.; de Bruijn, A. D.; McLaughlin, C. K.; Lo, P. K.; Sleiman, H. F. *Angew. Chem.* **2011**, *50*, 4620–4623.
- (30) Hunter, C. A.; Anderson, H. L. *Angew. Chem., Int. Ed.* **2009**, *48*, 7488–7499.